2
B meson decays

In this chapter we briefly discuss about B meson decays within the framework of Effective Field Theory (EFT). In particular, we discuss decays induced by the quark level transition $b \to s l^+ l^-$ ($l = e,\, \mu$) and $b \to c\, l\, \bar{\nu}$ ($l = e,\, \mu,\, \tau$).

2.1 EFT approach

The intuitive idea behind effective theories is that one can calculate even without knowing the exact theory. For e.g., in order to design and construct bridges and buildings, the engineers are not supposed to the know about weak interactions or grand unified theories. The inputs required are Newtonian mechanics, theory of elasticity and fluid flow theories. This is because the engineering design depends on parameters which are relevant at the macroscopic scales of order meters and hence the details of short distance physics such as electroweak interactions, quantum gravity are not required.

In nature, several interesting phenomena occur over a wide range of energy, length, and time scales. For e.g., so far, we have been able to explore from microscopic scales as small as one billionth of the size of an atom (10^4 GeV in energy scale) to macroscopic scales as large as the size of our observable universe (10^{-42} GeV in energy scale). Given this huge range, it would have been almost impossible to do physics if all physical phenomena had taken place at the same scale. Owing to this separation of scales, one can use the approximation to set to infinity (zero) all scales that are much larger (smaller) than the typical energy E of the physical process of interest. In this approximation, physics at scales much different from E becomes irrelevant and can be safety neglected. If required, these effect can be reintroduced in perturbation theory. This strategy is adopted by physicists in all sub-domains. EFTs are a model building technique which implements the above strategy to construct a quantitative framework which enables precise calculation at a given scale. In high energy physics, EFT theories are usually constructed using hierarchies in the energy scales. However, other quantities such as lengths, times, velocities, momenta can also be used.

An EFT provides simplified description of an underlying physical theory. This is achieved by using appropriate degrees of freedom relevant at the energy scale of interest. For e.g., in most of the problems in nuclear physics, we deal with nucleons rather than quarks. Even though it is known that the nucleons are made up of quarks, at the relevant energy scales in nuclear physics, quarks cannot be considered as the dynamical degrees of freedom. Only when the probing energy is increased, these degrees of freedom become relevant. Therefore, nuclear interactions can be considered as the effective theory of strong interactions. Similarly, classical mechanics can be considered as effective theory of quantum and relativistic mechanics. For macroscopic particles moving with velocities much smaller than the speed of light, classic mechanics is the appropriate theory to explain the dynamics of the system. Therefore in some sense, the ideas of EFT are "obvious." However, implementing them in a mathematically consistent way within the framework of quantum field theory is not so apparent.

2.1.1 What is EFT?

Let's start with the big picture. The big picture is that "there is interesting picture at all scales." What EFT let us do is, it allows to tease out this interesting physics at all scales. So in particular, we can focus on a particular scale and find interesting physics there using the tool of EFT. Now this is a little different than how we have been studying physics. If we think about drawing a diagram from our freshman year till now about how we learned physics, it was not by kind of focusing in on individual particular scales, but more from a kind of bottom-up point of view. So let us draw a picture of how we study physics (see Fig. 2.1).

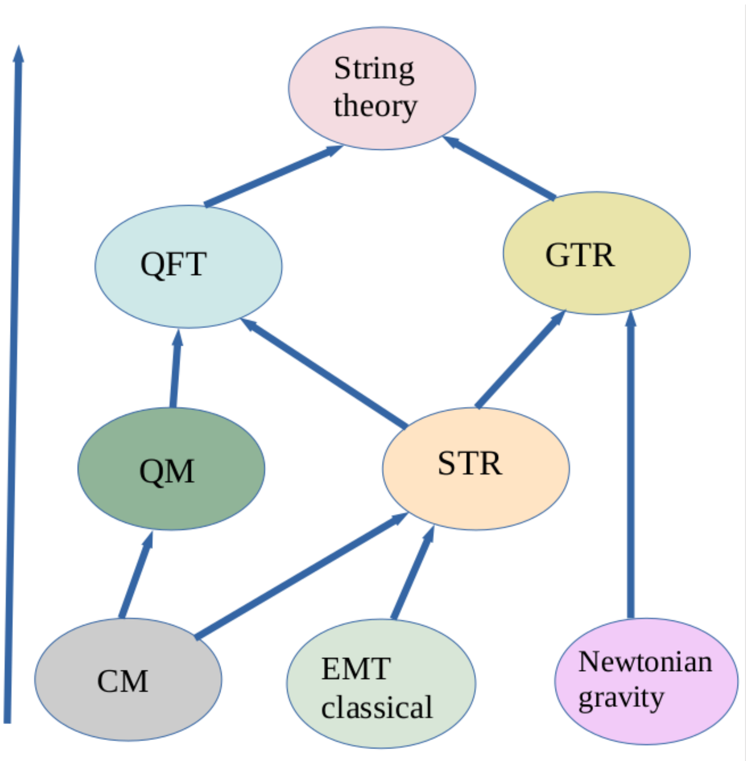

Figure 2.1: Bottom-up approach of learning physics.

We start with classical mechanics (CM), classical electromagnetic theory (EMT), Newtonian gravity and then we build on these things. So we learn quantum mechanics (QM) which builds on CM and special theory of relativity (STR) which is building on both CM and EMT. At some point we learn general theory of relativity (GTR) and quantum field theory (QFT). GTR builds upon STR and Newtonian gravity whereas QFT synthesize, say string theory.

What we do in EFT is exact opposite of that. We are going to be taking one of the blobs in Fig. 2.1, in particular QFT, and we will be looking deep inside it trying to make more and more specific field theories, i.e., we will be taking QFT or perhaps derivatives of it and figuring out how to take a very general theory, like QFT for the SM, and finding things that are more specific and in some ways more powerful than just having the original theory we started with - more powerful in the sense of being able to do calculations. So why do we want to do that. There's a couple of different reasons:

- As we go up in the chart presented in Fig. 2.1, it becomes more beautiful as we can write down a synthesis of physics in fewer lines but it also becomes harder to compute things. For e.g., if we just wanted to compute the energy spectrum of hydrogen, and we know very well that we can do that in QM. And particularly it's a classic example, and fairly easy. However, if we try to do that in QFT, it's much harder because QFT, in some sense, has too much for that problem. Another is the elliptical orbits of the planets, which are easier in Newtonian gravity than in GTR. There are many more examples.

- EFT allows us to compute more accurately in a simple fashion. So what we want when we think about EFT is we want the simplest frame work that captures the essential physics. We don't want to carry along for the ride a whole bunches of superfluous things that are not important for the problem we are trying to deal with. But we also don't want to give up anything. So even if we are giving up something in our leading order description, we want to retain the ability to correct that leading order description - order by order in some expansions. So that we can make it as precise as we desire i.e., we can correct it, in principle, to arbitrary precision. So what we are doing is that we are taking QFT and we are expanding it. And the lowest order determine that description is an EFT and that EFT may have different fields. It may have different symmetries. And it certainly have ability to calculate in a different fashion than the original theory. But we will keep higher order terms in that expansion and therefore, we will be able to correct it to arbitrary precision just by expanding to higher and higher order.

So some examples of this are non-relativistic expansion of QFT to non-relativistic QM or doing a post-Newtonian expansion in GTR to go back towards Newtonian gravity. We don't have to stop at the first term, we can keep higher-order terms. And in that way, we can calculate, for e.g., energy levels in hydrogen atom using a non-relativistic framework that encodes all the ingredients of QFT. or we can look at orbits of planets and relativistic corrections and general relativistic corrections by expanding this theory.

2.1.2 Main ingredients of EFTs

So let's say that we picked a physical system and wanted to describe it. What are the things that we should do in order to develop an EFT?

- *Degrees of freedom:* The first thing we need to do is to figure what relevant degree of freedom are? What are the things that actually matters for the problem we want to study?

- *Symmetries:* The second step in building an EFT consists in identifying the symmetries that constrain the form of the effective action, and therefore the dynamics of the system. Symmetries can come in many different flavors: they can be global, gauged, accidental, spontaneously broken, anomalous, approximate, contracted, etc. EFT may have more symmetry than the theory we started with. This is because we have neglected something, so we could have more symmetry.

- *Expansion parameters:* To figure out expansion parameters along with leading order description of the theory. For example, in particle physics these expansion parameters are usually ratios of energy scales E/Λ, where E is the characteristic energy scale of the process of interested in, and Λ is the typical energy scale of the UV physics one is neglecting. The expansion parameters may also include ratios of velocities (e.g. v/c in a non-relativistic limit), angular momenta (as in a semi-classical expansion), or small dimensionless couplings. Observable quantities are calculated in perturbation theory as series in these small parameters.

For e.g. in the context of QFT, the first point implies what fields we are using? The symmetry is basically guiding about interactions. If we have gauge symmetry, than of course we are going to write down something we respects that symmetry this will tell us something about the interaction terms. And finally these expansion parameters goes under the rubric of what is called power counting, meaning that we should be able to assign a definite order in the expansion parameter to each term in the effective action. This ensures that only a finite number of terms contribute at any given order in perturbation theory, and that we can decide upfront which terms to keep in the action based on the desired level of accuracy. If we have these three things together and we figure out the leading order description, then we have an EFT. For more details about the most commonly used EFTs in high energy physics, see for e.g., [145–148].

2.1.3 An example: Fermi theory of β decay

Let us consider the weak decays of B mesons within the context of standard model (SM). The weak decays of B mesons occur at the scale of the mass of b quark which is $\sim$ 5 GeV. The SM contains heavy degrees of freedom such as t quark, W or Z bosons having mass $\mathcal{O}(100)$ GeV. As we are interested in the effects of the heavy particles at energies which are much smaller than their masses, we can integrate them out and use the resulting effective Lagrangian. Therefore, it is useful to construct an effective theory from the full theory of electroweak interactions where the heavy degrees of freedom do not appear explicitly. This on one hand allows simplification of the analysis and on other hand enables us to zoom into the scale at which the given process occurs. Further, depending upon the required precision, one can always include higher order terms. This can be demonstrated using the theory of β decay proposed by Enrico Fermi.

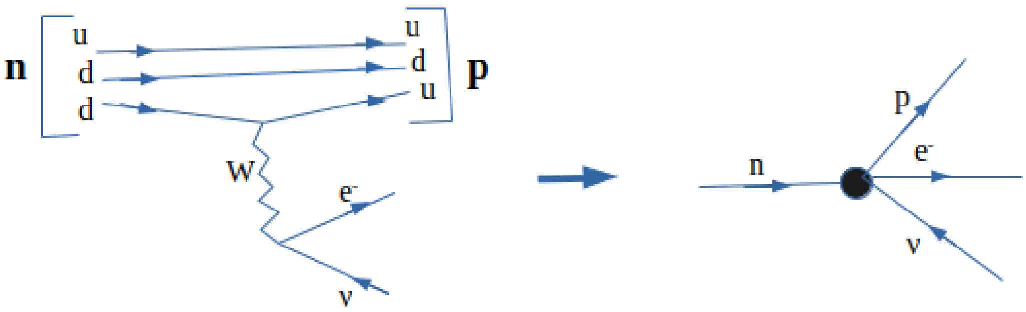

Figure 2.2: Left panel corresponds to the Feynman diagram of β decay in the full theory whereas the right panel represents the effective four-fermion interaction of β decay in EFT.

The β decay $n \to pe^-\bar{\nu}_e$ is induced by the charged current transition $d \to ue^-\bar{\nu}_e$. This interaction occurs at the tree level within the SM. The Feynman diagram for β decay in the full theory is shown in left panel of Fig. 2.2. The SM amplitude corresponding to this diagram is

$$-i\mathcal{M} = \left(\frac{ig}{2\sqrt{2}}\right)^2 V_{ud}\,[\bar{u}\gamma^\mu(1-\gamma_5)d]\left[\frac{-ig_{\mu\nu}}{k^2-m_W^2}\right][\bar{e}\gamma^\nu(1-\gamma_5)\nu_e] \tag{2.1}$$

Here, the maximum momentum transferred through the propagator is $k^2 = (m_d - m_u)^2$ which is very small compared to the mass of W boson m_W^2. Hence, the following approximation is justified

$$\frac{1}{k^2-m_W^2} \simeq -\frac{1}{m_W^2}, \quad k^2 << m_W^2. \tag{2.2}$$

In view of the above approximation, the amplitude can be written as

$$\mathcal{M} = \frac{g^2}{8m_W^2}V_{ud}\,[\bar{u}\gamma^\mu(1-\gamma_5)d]\,[\bar{e}\gamma_\mu(1-\gamma_5)\nu_e] + \mathcal{O}(\frac{k^2}{m_W^2}). \tag{2.3}$$

The $\mathcal{O}(k^2/m_W^2)$ terms in the above amplitude can be safely neglected and the local effective Hamiltonian for the β decay process can be written as

$$\mathcal{H}_{\text{eff}} = \frac{G_F}{\sqrt{2}}V_{ud}\,[\bar{u}\gamma^\mu(1-\gamma_5)d]\,[\bar{e}\gamma_\mu(1-\gamma_5)\nu_e]\,. \tag{2.4}$$

Here $G_F/\sqrt{2} = g^2/8m_W^2$ is the effective weak coupling known as Fermi constant. The above effective Hamiltonian corresponds to a four point interaction with strength $\sim G_F$. The diagram for this four point interaction is shown in right panel of Fig. 2.2. Thus we see that the the heavy propagator has now disappeared in the low energy process. In fact it is hidden in the effective coupling G_F.

Here it should be emphasize that one can have higher dimensional operators on the r.h.s of Eq. (2.4) corresponding to the terms $\mathcal{O}(k^2/m_W^2)$ in Eq. (2.3). These higher dimensional operators are actually the

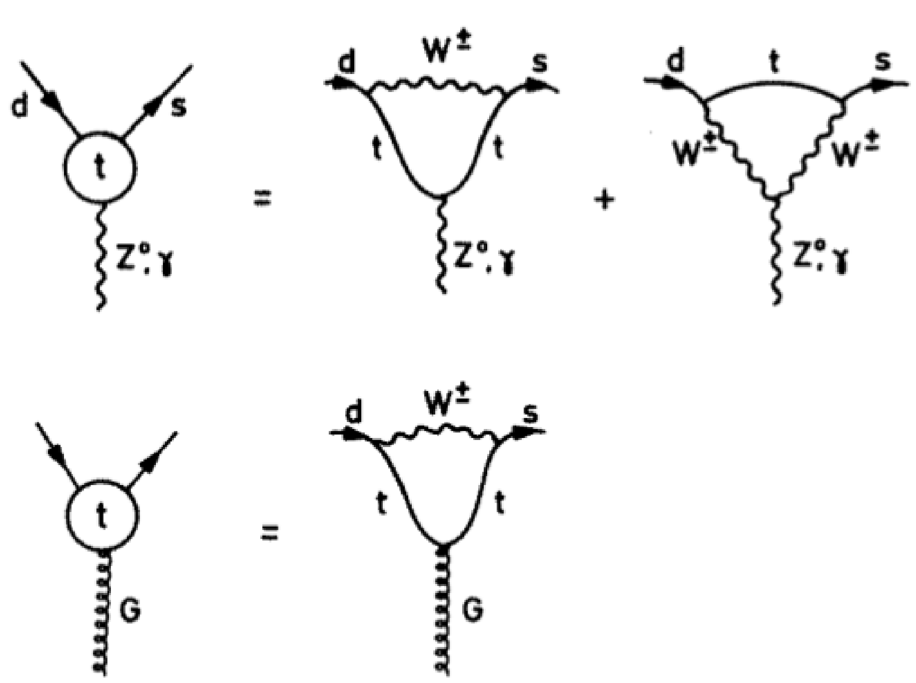

Figure 2.3: Penguin vertices resolved in terms of elementary vertices [149].

derivatives of the dimension-6 operator. Depending upon the requires precision, these higher dimension operators can be included the analysis. This forms the basis of operator product expansion (OPE) where we generally expand the product of two charged current operators into a series of effective local operators. An effective coupling constant, known as Wilson coefficient (WC), is associated with each of these local operators. These WCs measure the strength of the corresponding operator. From Eq. (2.4), it is obvious that in the β decay, the leading local effective operator is a dimension-6 operator with the WC equal to one.

In a similar way, SM can be considered an effective theory of new physics construed at a scale much higher than the weak energy scale. In many of the new physics models, SM can be recovered in the low energy scale limit through the decoupling of the heavy particles that have a mass much larger than the weak scale. The effects of physics at higher energy scales can be parametrized with effective operators and their associated coefficients at a given energy scale. Therefore, even if new heavy particles remain unobserved at the current collider facilities, the EFT formalism allows probing of new physics through corrections to the SM observables which are added in an expansion in the inverse power of the new physics scale after the new particles have been integrated out from the theory.

We now discuss this formalism in the context of B decays.

2.2 Effective Hamiltonian for B decays

Owing to Glashow–Iliopoulos–Maiani (GIM) mechanism, flavour changing neutral current (FCNC) interactions do not occur at the tree level in the SM. They can only occur at the loop level via $W^\pm$ vertex. The effective operators for FCNC processes are obtained by calculating penguin and box diagrams by resolving them in terms of basic vertices as shown Fig. 2.3 and Fig. 2.4, respectively.

These effective operators for strangeness changing processes are given by [149]:

$$\mathrm{Box}(\Delta S = 2) \; = \; \sum_i \lambda_i^2 \frac{G_{\mathrm{F}}^2}{16\pi^2} M_W^2 S_0(x_i)(\bar{s}d)_{V-A}(\bar{s}d)_{V-A} \tag{2.5}$$

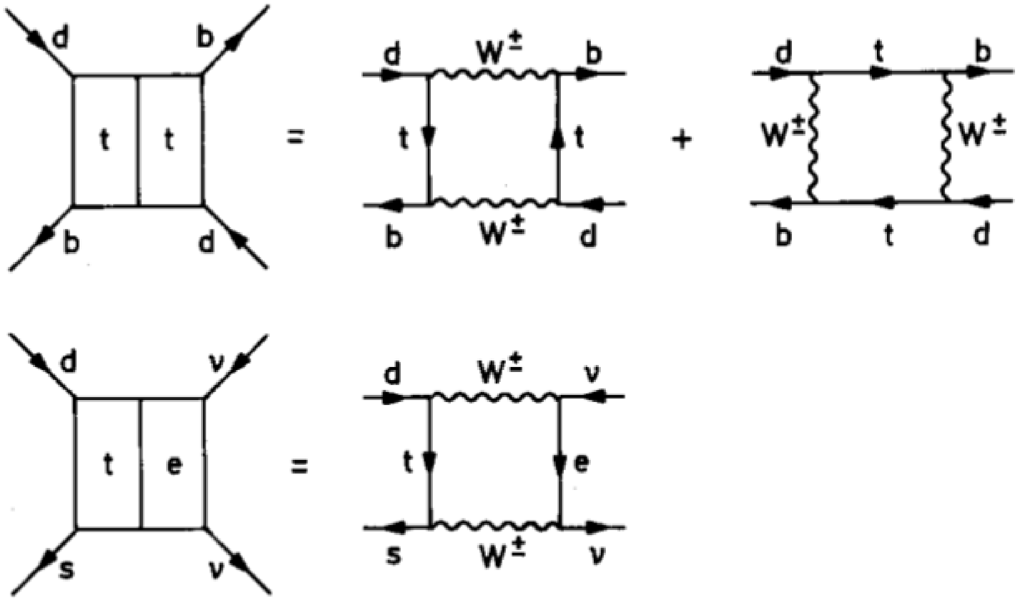

Figure 2.4: Box vertices resolved in terms of elementary vertices [149].

$$\mathrm{Box}(T_3 = 1/2) \;=\; \sum_i \lambda_i \frac{G_\mathrm{F}}{\sqrt{2}} \frac{\alpha}{2\pi \sin^2\theta_\mathrm{W}} [-4B_0(x_i)](\bar{s}d)_{V-A}(\bar{\nu}\nu)_{V-A} \tag{2.6}$$

$$\mathrm{Box}(T_3 = -1/2) \;=\; \sum_i \lambda_i \frac{G_\mathrm{F}}{\sqrt{2}} \frac{\alpha}{2\pi \sin^2\theta_\mathrm{W}} B_0(x_i)(\bar{s}d)_{V-A}(\bar{\mu}\mu)_{V-A} \tag{2.7}$$

$$\bar{s}Zd \;=\; \sum_i i\lambda_i \frac{G_\mathrm{F}}{\sqrt{2}} \frac{e}{2\pi^2} M_Z^2 \frac{\cos\theta_\mathrm{W}}{\sin\theta_\mathrm{W}} C_0(x_i)\bar{s}\gamma_\mu(1-\gamma_5)d\varepsilon_Z^\mu \tag{2.8}$$

$$\bar{s}\gamma d \;=\; -\sum_i i\lambda_i \frac{G_\mathrm{F}}{\sqrt{2}} \frac{e}{8\pi^2} D_0(x_i)\bar{s}(q^2\gamma_\mu - q_\mu \not{q})(1-\gamma_5)d\varepsilon^\mu \tag{2.9}$$

$$\bar{s}G^a d \;=\; -\sum_i i\lambda_i \frac{G_\mathrm{F}}{\sqrt{2}} \frac{g_s}{8\pi^2} E_0(x_i)\bar{s}_\alpha(q^2\gamma_\mu - q_\mu \not{q})(1-\gamma_5)T^a_{\alpha\beta}d_\beta\varepsilon_G^\mu \tag{2.10}$$

$$\bar{s}\gamma' d \;=\; \sum_i i\bar{\lambda}_i \frac{G_\mathrm{F}}{\sqrt{2}} \frac{e}{8\pi^2} D_0'(x_i)\bar{s}[i\sigma_{\mu\lambda}q^\lambda[m_b(1+\gamma_5)]]d\varepsilon^\mu \tag{2.11}$$

$$\bar{s}G'^a d \;=\; \sum_i i\bar{\lambda}_i \frac{G_\mathrm{F}}{\sqrt{2}} \frac{g_s}{8\pi^2} E_0'(x_i)\bar{s}_\alpha[i\sigma_{\mu\lambda}q^\lambda[m_b(1+\gamma_5)]]T^a_{\alpha\beta}d_\beta\varepsilon_G^\mu\,. \tag{2.12}$$

Here $\lambda_i = V_{is}^* V_{id}$ and q_μ is the momenta of outgoing gluon or photon whereas $\varepsilon^\mu, \varepsilon_Z^\mu, \varepsilon_G^\mu$ are the polarization vectors of photon, Z and gluon, respectively. The matrix elements of FCNC processes can be calculated by making use of these effective operators. These processes are governed by a set of gauge independent basic structure functions [149]: $S_0(x_i), X_0(x_i), Y_0(x_i), Z_0(x_i), E_0(x_i), D_0^{'}(x_), E_0^{'}(x_i)$. Running on the same lines, one can write operators for $\bar{b}d, \bar{b}s$ and $\bar{c}u$ processes.

The effective Hamiltonian for the decay of a B meson can be written as

$$\mathcal{H}_{eff} = \sum_k C_k O_k. \tag{2.13}$$

Here O_k denotes the operators such as $(\bar{s}d)_{V-A}(\bar{s}d)_{V-A}, (\bar{s}d)_{V-A}(\bar{u}u)_{V-A}$ etc. The Wilson coefficients C_k are simply the linear combination of the various structure functions listed above. These operators play very important role in the phenomenology of weak decays and are classified into six categories [150]:

Current-Current Operators (Fig. 2.5 (a)) :

$$Q_1 = (\bar{c}_\alpha b_\beta)_{\rm V-A}\,(\bar{s}_\beta c_\alpha)_{\rm V-A} \qquad Q_2 = (\bar{c}b)_{\rm V-A}\,(\bar{s}c)_{\rm V-A} \tag{2.14}$$

QCD-Penguins Operators (Fig. 2.5 (b)) :

$$Q_3 = (\bar{s}b)_{\rm V-A}\sum_q (\bar{q}q)_{\rm V-A} \qquad Q_4 = (\bar{s}_\alpha b_\beta)_{\rm V-A}\sum_q (\bar{q}_\beta q_\alpha)_{\rm V-A} \tag{2.15}$$

$$Q_5 = (\bar{s}b)_{\rm V-A}\sum_q (\bar{q}q)_{\rm V+A} \qquad Q_6 = (\bar{s}_\alpha b_\beta)_{\rm V-A}\sum_q (\bar{q}_\beta q_\alpha)_{\rm V+A} \tag{2.16}$$

Electroweak-Penguins Operators (Fig. 2.5 (c)) :

$$Q_7 = \frac{3}{2}\,(\bar{s}b)_{\rm V-A}\sum_q e_q\,(\bar{q}q)_{\rm V+A} \qquad Q_8 = \frac{3}{2}\,(\bar{s}_\alpha b_\beta)_{\rm V-A}\sum_q e_q\,(\bar{q}_\beta q_\alpha)_{\rm V+A} \tag{2.17}$$

$$Q_9 = \frac{3}{2}\,(\bar{s}b)_{\rm V-A}\sum_q e_q\,(\bar{q}q)_{\rm V-A} \qquad Q_{10} = \frac{3}{2}\,(\bar{s}_\alpha b_\beta)_{\rm V-A}\sum_q e_q\,(\bar{q}_\beta q_\alpha)_{\rm V-A} \tag{2.18}$$

Magnetic-Penguins Operators (Fig. 2.5 (d)) :

$$Q_{7\gamma} = \frac{e}{8\pi^2} m_b \bar{s}_i \sigma^{\mu\nu}(1+\gamma_5) b_i F_{\mu\nu} \qquad Q_{8G} = \frac{g}{8\pi^2} m_b \bar{s}_i \sigma^{\mu\nu}(1+\gamma_5) T^a_{ij} b_j G^a_{\mu\nu} \tag{2.19}$$

$\Delta S = 2$ and $\Delta B = 2$ Operators (Fig. 2.5 (e)) :

$$Q(\Delta S = 2) = (\bar{s}d)_{V-A}(\bar{s}d)_{V-A} \qquad Q(\Delta B = 2) = (\bar{b}d)_{V-A}(\bar{b}d)_{V-A} \tag{2.20}$$

Semi-Leptonic Operators (Fig. 2.5 (f)) :

$$Q_{7V} = (\bar{s}b)_{V-A}(\bar{e}e)_V \qquad Q_{7A} = (\bar{s}b)_{V-A}(\bar{e}e)_A \tag{2.21}$$

$$Q_{9V} = (\bar{b}s)_{V-A}(\bar{e}e)_V \qquad Q_{10A} = (\bar{b}s)_{V-A}(\bar{e}e)_A \tag{2.22}$$

$$Q(\bar{\nu}\nu) = (\bar{s}b)_{V-A}(\bar{\nu}\nu)_{V-A} \qquad Q(\bar{\mu}\mu) = (\bar{s}b)_{V-A}(\bar{\mu}\mu)_{V-A} \tag{2.23}$$

As the decays are observed only at the hadronic level, we have to use the OPE technique to calculate an amplitude for a hadronic decay. The amplitude for a hadronic decay $A \to B$ can be written as

$$\mathcal{M}(A \to B) = \langle B|\mathcal{H}_{\rm eff}|A\rangle = \frac{G_F}{\sqrt{2}}\sum_i V^i_{\rm CKM} C_i(\mu)\langle B|\mathcal{O}_i(\mu)|A\rangle\,. \tag{2.24}$$

Here $\langle B|\mathcal{O}_i(\mu)|A\rangle$ is the hadronic matrix elements and $C_i(\mu)$ is the WC with a scale dependence of μ. The short distance (perturbative) effects are embedded in the WC whereas the hadronic matrix elements contain the long distance (non-perturbative) contributions. The hadronic matrix elements are parametrized in terms of the helicity amplitudes which depend on various form factors (FF). These FFs are calculated by using non-perturbative methods such as QCD sum rule, relativistic quark model, lattice QCD etc. In case of heavy flavours such as B meson, the heavy quark effective theory (HQET) is a quite useful tool to calculate the FFs.

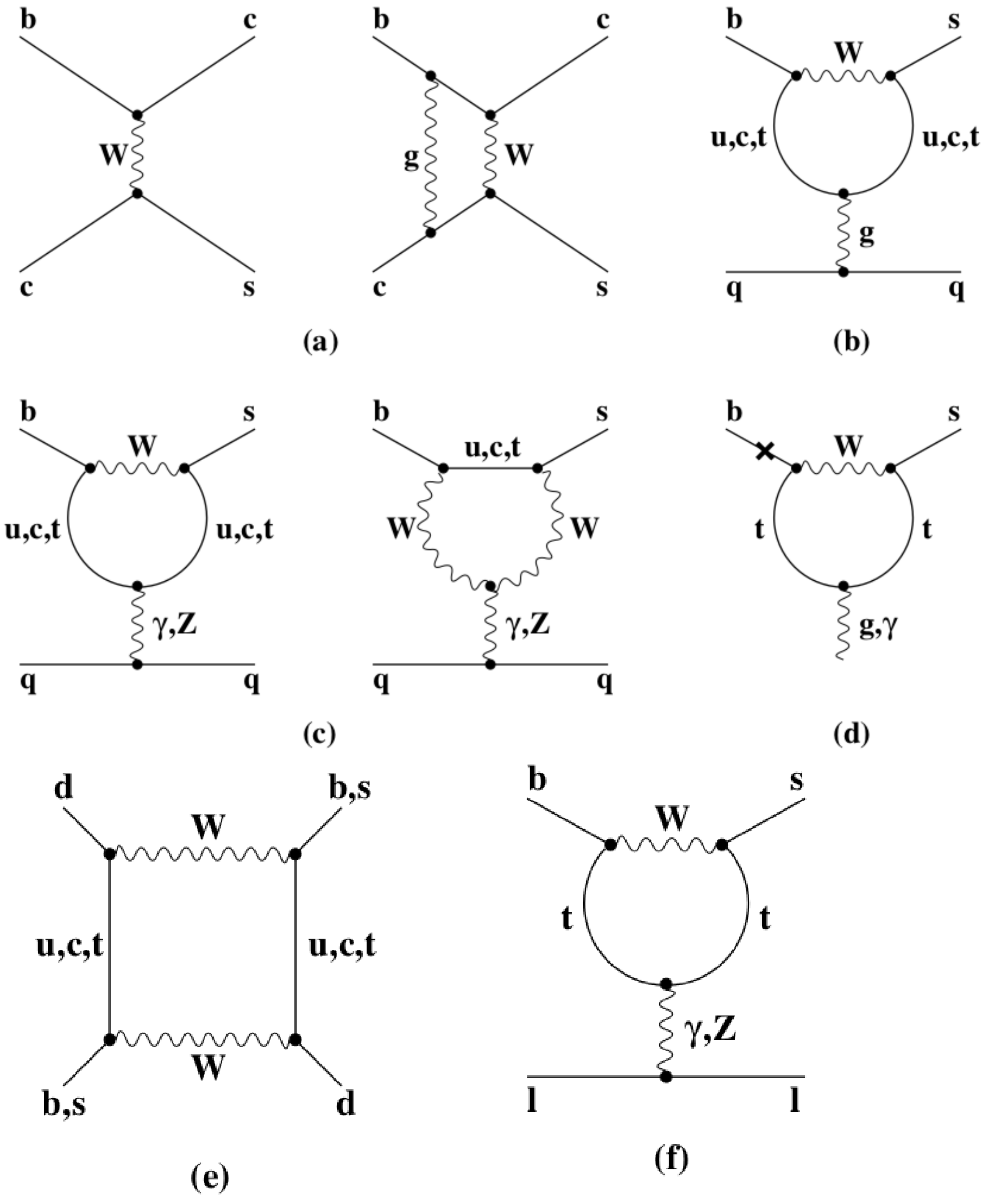

Figure 2.5: These are diagrams in the full theory [150]. In diagram (d), the cross represents a mass-insertion which shows that the magnetic penguins originate from the mass-term on the external line in the QCD or QED penguin diagrams.

2.3 Decays induced by quark level transition $b \to s\, l^+\, l^-$

The quark level interaction $b \to s\, l^+\, l^-$ is forbidden at the tree level in the SM and can occur only at the loop level. Therefore it can serve as an important tool to test higher order corrections to the SM and also explore physics beyond SM. Feynman diagrams in the SM for $b \to s\, l^+\, l^-$ quark level transition, without including QCD corrections, are depicted in Fig. 2.6.

This quark level transition induces various decays such as

- the semileptonic B decays $B \to (X_s,\, K,\, K^*)\, l^+\, l^-$,

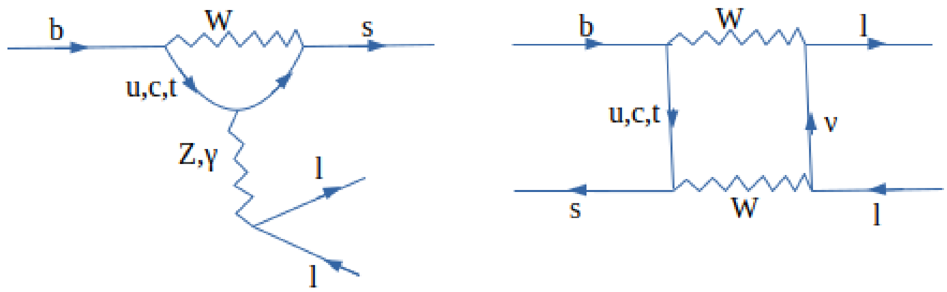

Figure 2.6: Feynman diagrams for $b \to s\, l^+\, l^-$ transition with in the SM.

- the purely leptonic decay $B_s \to l^+\, l^-$,
- the semileptonic B_s decay $B_s \to \phi\, l^+\, l^-$.

Therefore $b \to s\, l^+\, l^-$ transition provides a large number of observables to explore new physics. The effective Hamiltonian for $b \to s\, l^+\, l^-$ in the SM can be written as

$$\mathcal{H}_{eff} = -\frac{4G_F}{\sqrt{2}} V_{ts} V_{tb}^* \sum_{i=1}^{10} C_i(\mu)\, O_i(\mu)\ , \tag{2.25}$$

where the operators O_i and corresponding Wilson coefficients C_i are given in Ref. [151]. The WCs C_i which encode the short distance physics is a scale dependent quantity. These WCs are calculated at matching scale $\mu = m_W$ in a perturbative expansion of $\alpha_s(m_W)$. However, as the physical processes occur at the scale m_b, hence μ has to be evaluated at the m_b scale using the renormalization group (RG) equations. The WCs can be expanded as

$$C_i = C_i^0 + \frac{\alpha_s}{4\pi} C_i^{(1)} + \big(\frac{\alpha_s}{4\pi}\big)^2 C_i^{(2)} + \mathcal{O}(\alpha_s^3)\,,$$

where $C_i^{(0)}$ is the tree level contribution which is non-zero only for the O_2 operator. The matching conditions at $\mu = m_W$ have been calculated with two loop accuracy [152] for which one needs to include the anomalous degrees of freedom in RG equations up to an accuracy of three loops. The calculations of these anomalous dimensions, within SM, can be found in Ref. [153, 154]. The O_9 operator mixes with the $O_{1,...,6}$ operators through the diagrams mediated by virtual photon decaying into a lepton pair. Moreover, the operator O_7 also gets modified by these operators. Therefore the effective WCs take the following forms after RG evolutions [155]:

$$\begin{aligned}
C_7^{eff} &= \frac{4\pi}{\alpha_s} C_7 - \frac{1}{3} C_3 - \frac{4}{9} C_4 - \frac{20}{3} C_5 - \frac{80}{9} C_6,\\
C_8^{eff} &= \frac{4\pi}{\alpha_s} C_8 + C_3 - \frac{1}{6} C_4 + 20 C_5 - \frac{10}{3} C_6,\\
C_9^{eff} &= \frac{4\pi}{\alpha_s} C_9 + Y(q^2),\\
C_{10}^{eff} &= \frac{4\pi}{\alpha_s} C_{10},
\end{aligned}$$

with

$$\begin{aligned}
Y(q^2) = {} & h(q^2, m_c)\big(\frac{4}{3} C_1 + C_2 + 6C_3 + 60C_5\big) - \frac{1}{2} h(q^2, m_b)\big(7C_3 + \frac{4}{3} C_4 + 76C_5 + \frac{64}{3} C_6\big)\\
& - \frac{1}{2} h(q^2, 0)\big(C_3 + \frac{4}{3} C_4 + 16C_5 + \frac{64}{3} C_6\big) + \frac{4}{3} C_3 + \frac{64}{9} C_5 + \frac{64}{27} C_6.
\end{aligned}$$

The function h is defined as

$$h(q^2, m_b) = -\frac{4}{9}\left(\ln\frac{m_q^2}{\mu^2} - \frac{2}{3} - z\right) - \frac{4}{9}(2+z)\sqrt{|z-1|} \times \begin{cases} \arctan\frac{1}{\sqrt{z-1}}, & z > 1 \\ \ln\frac{1+\sqrt{1-z}}{\sqrt{z}} - \frac{i\pi}{2}, & z \leq 1 \end{cases},$$

where $z = \frac{4m_q^2}{q^2}$.

In the following we discuss various decays in the $b \to s l^+ l^-$ sector.

2.3.1 Inclusive semileptonic decay $B \to X_s\, l^+ l^-$

The differential decay rate for $B \to X_s\, l^+ l^-$ within SM is given by

$$\begin{aligned}\frac{d\mathcal{B}(B \to X_s l^+ l^-)}{d\hat{s}} &= \mathcal{B}(B \to X_c l\bar{\nu})\frac{\alpha^2}{4\pi^2 f(z)\kappa(z)}\frac{|V_{tb}V_{ts}^*|^2}{|V_{cb}|^2}(1-\hat{s})^2\sqrt{1-\frac{4\hat{m_l}^2}{\hat{s}}} \\ &\times\Big[|C_9^{eff}|^2(1+\frac{2\hat{m_l}^2}{\hat{s}})(1+2\hat{s}) + 4|C_7^{eff}|^2(1+\frac{2\hat{m_l}^2}{\hat{s}})(1+\frac{2}{\hat{s}}) \\ &+|C_{10}|^2[(1+2\hat{s}) + \frac{2\hat{m_l}^2}{\hat{s}}(1-4\hat{s})] \\ &+12Re(C_7^{eff}C_9^{eff*}(1+\frac{2\hat{m_l}^2}{\hat{s}}))\Big]. \end{aligned} \tag{2.26}$$

Here $\hat{m_i} = m_/m_{b,pole}$, $\hat{s} = s/m^2_{b,pole}$ and $z = m_c^2/m_b^2$. Further, $f(z)$ and $\kappa(z)$ represent the phase space and QCD corrections [156], respectively. As, within SM, $B \to X_s\, l^+ l^-$ occurs at the loop level with diagrams mediated by γ and Z boson, the semi-leptonic operators O_7, O_9 and O_{10} are relevant for this decay mode. The decay mode $B \to X_s\, l^+ l^-$ has relatively small theoretical uncertainties as compared to the exclusive decay counterparts. As far as experiments are concerned, the inclusive decays are less readily accessible.

2.3.2 Exclusive semileptonic decay $B \to K\, l^+ l^-$

The effective Hamiltonian for $B \to K\, \mu^+ \mu^-$ is the same as that of $B \to X_s\, l^+ l^-$. The $B \to K$ matrix element, $\mathcal{M}(B \to K l^+ l^-) = \langle l(p_-)\bar{l}(p_+)K(p_K)|\mathcal{H}_{eff}|\bar{B}(p_B)\rangle$, can be parameterized in terms of form factors

$$\begin{aligned}\langle K(p_K)|\bar{s}\gamma_\mu b|\bar{B}(p_B)\rangle &= (2p_B - q)_\mu f_+(q^2) + \frac{m_B^2 - m_K^2}{q^2}q_\mu\big[f_0(q^2) - f_+(q^2)\big], \\ \langle K(p_K)|\bar{s}i\sigma_{\mu\nu}q^\nu b|\bar{B}(p_B)\rangle &= -\big[(2p_B - q)_\mu q^2 - (m_B^2 - m_K^2)q_\mu\big]\frac{f_T(q^2)}{m_B + m_K}, \end{aligned} \tag{2.27}$$

where $q = (p_+ + p_-)$. In the large recoil region, matrix element can be calculated using QCD factorization [157, 158]. In high-q^2 region, this decay can be studied by operator product expansion (OPE) with the use of improved Isgur-Wise form factor relations.

These form factors can be related to a single form factor $\xi_P(q^2)$ in the leading order in (1/E) expansion. A factorization scheme is chosen with $f_+(q^2) = \xi_P(q^2)$ [159] within QCD factorization. The form factors obey the following symmetry relations [159, 160]

$$\begin{aligned}\frac{f_0}{f_+} &= \frac{2E}{m_B}\big[1 + \mathcal{O}(\alpha_s) + \mathcal{O}(\frac{q^2}{m_B^2}\sqrt{\frac{\Lambda_{QCD}}{E}})\big], \\ \frac{f_T}{f_+} &= \frac{m_B + m_K}{m_B}\big[1 + \mathcal{O}(\alpha_s) + \mathcal{O}(\sqrt{\frac{\Lambda_{QCD}}{E}})\big]. \end{aligned} \tag{2.28}$$

The form factor $f_+(q^2) = \xi_P(q^2)$ is taken from light cone sum rule (LCSR) calculations [161]. Using the QCD factorization results, matrix element can be written as

$$\mathcal{M}(B \to K l^+ l^-) = i \frac{G_F \alpha_e}{\sqrt{2}\pi} V_{tb} V_{ts}^* \xi_P(q^2) \big[F_V p_B^\mu (\bar{l}\gamma_\mu l) + F_A p_B^\mu (\bar{l}\gamma_\mu \gamma_5 l) + F_P \bar{l}\gamma_5 l \big]. \tag{2.29}$$

The functions $F_i = F_i(q^2)(i = V, A, P)$ are defined as

$$F_A = C_{10}, \tag{2.30}$$

$$F_V = C_9 + \frac{2m_b}{m_B} \frac{\mathcal{T}_P(q^2)}{\xi_P(q^2)}, \tag{2.31}$$

$$F_P = m_l C_{10} \big[\frac{m_B^2 - m_K^2}{q^2} \big(\frac{f_0(q^2)}{f_+(q^2)} - 1 \big) - 1 \big], \tag{2.32}$$

where the amplitude $\mathcal{T}_P$ is defined in Ref. [158]. The decay rate of $B \to K l^+ l^-$ in SM can be given as

$$\Gamma_l^{\rm SM} = \frac{\Gamma_0}{3} \int_{q^2_{\rm min}}^{q^2_{\rm max}} dq^2 \, \xi_P^2(q^2) \lambda^{3/2} (|F_A|^2 + |F_V|^2) \tag{2.33}$$

$$\times \left\{ 1 + \mathcal{O}\left(\frac{m_l^4}{q^4} \right) + \frac{m_l^2}{M_B^2} \times \mathcal{O}\left(\alpha_s, \frac{q^2}{M_B^2} \sqrt{\frac{\Lambda_{QCD}}{E}} \right) \right\},$$

where

$$\Gamma_0 = \frac{G_F^2 \alpha_e^2 |V_{tb} V_{ts}^*|^2}{512 \pi^5 m_B^3}, \tag{2.34}$$

$$\lambda = m_B^4 + m_K^4 + q^4 - 2(m_B^2 m_K^2 + m_B^2 q^2 + m_K^2 q^2). \tag{2.35}$$

Here m_B and m_K are the masses of B and K meson, respectively.

In high-q^2 region this decay can be studied by operator product expansion (OPE) with the use of improved Isgur-Wise form factor relations. The QCD operator identity [162, 163]

$$i\partial^\nu (\bar{s}\, i\sigma_{\mu\nu}\, b) = i\partial_\mu (\bar{s} b) - m_b (\bar{s}\, \gamma_\mu\, b) - 2(\bar{s}\, i\, \overleftarrow{D}_\mu\, b), \tag{2.36}$$

allows us to derive an improved Isgur-Wise relation between f_T and f_+,

$$f_T(q^2, \mu) = \frac{m_B\,(m_B + m_K)}{q^2} [\kappa(\mu) f_+(q^2) + \frac{2\, \delta_+^{(0)}(q^2)}{m_B}] + \mathcal{O}\left(\alpha_s \frac{\Lambda}{m_b}, \frac{\Lambda^2}{m_b^2} \right), \tag{2.37}$$

$$= \frac{m_B\,(m_B + m_K)}{q^2} \, \kappa(\mu)\, f_+(q^2) + \mathcal{O}\left(\frac{\Lambda}{m_b} \right), \tag{2.38}$$

where $\delta_+^{(0)}(q^2)$ is the Heavy Quark Effective Theory (HQET) form factor which is defined in [162]. The μ-dependent coefficient κ is given by

$$\kappa(\mu) = (1 + 2\, \frac{D_0^{(v)}(\mu)}{C_0^{(v)}(\mu)}) \frac{m_b(\mu)}{m_B}. \tag{2.39}$$

which includes $\mathcal{O}(\alpha_s)$ corrections. The HQET Wilson coefficients $C_0^{(v)}, D_0^{(v)}$ are given in [163].

The form factors are parameterized as [164]

$$f_i(s) = \frac{f_i(0)}{1 - s/m^2_{{\rm res},i}} \{ 1 + b_1^i \left(z(s) - z(0) + \frac{1}{2} \left(z(s)^2 - z(0)^2 \right) \right) \}, \quad s = q^2, \tag{2.40}$$

$$z(s) = \frac{\sqrt{\tau_+ - s} - \sqrt{\tau_+ - \tau_0}}{\sqrt{\tau_+ - s} + \sqrt{\tau_+ - \tau_0}}, \quad \tau_0 = \sqrt{\tau_+} \left(\sqrt{\tau_+} - \sqrt{\tau_+ - \tau_-} \right), \quad \tau_\pm = (m_B \pm m_K)^2 \,,$$

where $i = +, T, 0$. The values of $f_i(q^2 = 0)$ are taken from LCSR calculations. Input to the $B \to K$ form factor parameterization are taken from Ref. [164].

2.3.3 Exclusive semileptonic decay $B \to K^* l^+ l^-$

The decay $B \to K^* l^+ l^-$ provides plethora of observables to probe new physics. The complete angular distribution for the decay $B \to K^* l^+ l^-$ is described by four independent kinematic variables: the lepton-pair invariant mass squared q^2, two polar angles θ_μ and θ_K and the angle ϕ between the planes of the dimuon and $K\pi$ decays, as shown in Fig. 2.7.

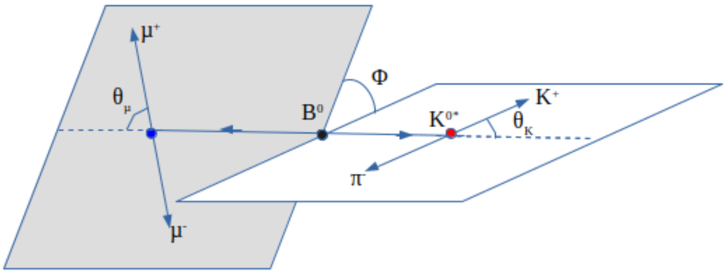

Figure 2.7: The description of the polar angles θ_μ, θ_K and ϕ in the angular distribution of $B^0 \to K^{*0}(K^+\pi^-)\mu^+\mu^-$ decay.

The differential decay distribution of $B \to K^* l^+ l^-$ decay can be written as

$$\frac{d^4\Gamma(B \to K^*(\to K\pi)l^+ l^-)}{dq^2\, d\cos\theta_l\, d\cos\theta_K\, d\phi} = \frac{9}{32\pi} J(q^2, \theta_l, \theta_K, \phi)\,. \tag{2.41}$$

where

$$\begin{aligned} J(q^2, \theta_l, \theta_K, \phi) = {} & J_{1s}\sin^2\theta_K + J_{1c}\cos^2\theta_K + (J_{2s}\sin^2\theta_K + J_{2c}\cos^2\theta_K)\cos 2\theta_l \\ & + J_3 \sin^2\theta_K \sin^2\theta_l \cos 2\phi + J_4 \sin 2\theta_K \sin 2\theta_l \cos\phi \\ & + J_5 \sin 2\theta_K \sin\theta_l \cos\phi + (J_{6s}\sin^2\theta_K + J_{6c}\cos^2\theta_K)\cos\theta_l \\ & + J_7 \sin 2\theta_K \sin\theta_l \sin\phi + J_8 \sin 2\theta_K \sin 2\theta_l \sin\phi + J_9 \sin^2\theta_K \sin^2\theta_l \sin 2\phi\,. \end{aligned} \tag{2.42}$$

In the limit of neglecting lepton mass, the J_i's depend on the six K^* spin amplitudes $A_\parallel^{L,R}$, $A_\perp^{L,R}$, $A_0^{L,R}$. For massive leptons, these J_i's depend on one more additional complex amplitude A_t. For example,

$$J_{1s} = \frac{(2+\beta_l^2)}{4}[|A_\perp^L|^2 + |A_\parallel^L|^2 + |A_\perp^R|^2 + |A_\parallel^R|^2] + \frac{4m_l^2}{q^2} Re(A_\perp^L A_\perp^{R*} + A_\parallel^L A_\parallel^{R*})\,. \tag{2.43}$$

We can now define the optimized observables like P_1, P_2, P_4', P_5', P_6', P_8' [165]:

$$\langle P_1 \rangle = \frac{1}{2}\frac{\int_{\text{bin}} dq^2[J_3 + \bar{J}_3]}{\int_{\text{bin}} dq^2[J_{2s} + \bar{J}_{2s}]}, \qquad \langle P_2 \rangle = \frac{1}{8}\frac{\int_{\text{bin}} dq^2[J_{6s} + \bar{J}_{6s}]}{\int_{\text{bin}} dq^2[J_{2s} + \bar{J}_{2s}]} \tag{2.44}$$

$$\langle P_3 \rangle = -\frac{1}{4}\frac{\int_{\text{bin}} dq^2[J_9 + \bar{J}_9]}{\int_{\text{bin}} dq^2[J_{2s} + \bar{J}_{2s}]} \qquad \langle P_4' \rangle = \frac{1}{\mathcal{N}'_{bin}}\int_{\text{bin}} dq^2[J_4 + \bar{J}_4]\,,, \tag{2.45}$$

$$\langle P_5' \rangle = \frac{1}{2\mathcal{N}'_{bin}}\int_{\text{bin}} dq^2[J_5 + \bar{J}_5]\,, \qquad \langle P_6' \rangle = -\frac{1}{2\mathcal{N}'_{bin}}\int_{\text{bin}} dq^2[J_7 + \bar{J}_7] \tag{2.46}$$

$$\langle P_8' \rangle = \frac{1}{\mathcal{N}'_{bin}}\int_{\text{bin}} dq^2[J_8 + \bar{J}_8] \tag{2.47}$$

where $\bar{J}_i$'s can be obtained from J_i's by all weak phases conjugated. The normalization factor is defined as

$$\mathcal{N}'_{bin} = \sqrt{-\int_{bin} dq^2[J_{2s} + \bar{J}_{2s}]\int_{\text{bin}} dq^2[J_{2c} + \bar{J}_{2c}]}\,. \tag{2.48}$$

The analysis of $B \to K^* l^+ l^-$ in the low-q^2 region is based on QCD factorization (QCDF) [158] and its quantum field-theoretical formulation, Soft-Collinear Effective Theory (SCET). The analysis of $B \to K^* l^+ l^-$ in the high-q^2 region is based on the heavy-quark effective theory framework [163]. The main sources of uncertainties in the low-q^2 region are:CKM elements, the form factors, the unknown $1/m_b$ subleading corrections, the quark masses and the renormalization scale μ_b. In the high-q^2 region, there is an additional correction of $\mathcal{O}(1/m_b)$ to the improved Isgur-Wise form factor relations.

2.3.4 Purely leptonic decay $B_s \to l^+ l^-$

The purely leptonic decay $B_s \to l^+ l^-$ is chirally suppressed within the SM and hence has a smaller branching ratio in comparison to that of the semileptonic decays induced by $b \to s l^+ l^-$ transition. Within the SM, $B_s \to l^+ l^-$ is dominated by the Z^0-penguin and box diagrams involving top quark. The SM prediction of branching ratio of $B_s \to \mu^+ \mu^-$ is $\sim 3 \times 10^{-9}$. This decay has been experimentally observed with a branching ratio close to the SM value [166, 167].

The branching ratio in the SM is given by

$$\mathcal{B}(B_s \to l^+ l^-) = \frac{G_F^2 \alpha^2 M_{B_s} m_\mu^2 f_{bs}^2 \tau_{B_s}}{16\pi^3} |V_{ts}^* V_{tb}|^2 \sqrt{1 - 4(m_l^2/M_{B_s}^2)} |C_{10}|^2 \,, \tag{2.49}$$

where f_{bs} is decay constant and τ_{B_s} is B_s meson lifetime.

2.4 Decays induced by quark level transition $b \to c\tau\bar{\nu}$

The quark level transition $b \to c\tau\bar{\nu}$ occurs at tree level in the SM, as shown in Fig. 2.8. Neglecting QCD effects, the SM amplitude for this diagram can be written as

$$-i\mathcal{M} = \left(\frac{ig}{2\sqrt{2}}\right)^2 V_{cb} \big[\bar{c}\gamma^\mu (1-\gamma_5) b\big] \left[\frac{-ig_{\mu\nu}}{q^2 - m_W^2}\right] \big[\bar{l}\gamma^\nu (1-\gamma^5)\nu_l\big].$$

With the same approximation as taken in β decay, $q^2 << m_W^2$, the SM effective Hamiltonian is obtained as

$$\begin{aligned}
H_{eff} &= \frac{G_F}{\sqrt{2}} V_{cb} \big[\bar{c}\gamma^\mu (1-\gamma_5) b\big] \big[\bar{l}\gamma^\nu (1-\gamma^5)\nu_l\big] + \mathcal{O}\Big(\frac{q^2}{m_W^2}\Big) \\
&= \frac{4G_F}{\sqrt{2}} V_{cb} \big[\bar{c}\gamma^\mu \frac{(1-\gamma^5)}{2} b\big] \big[\bar{l}\gamma^\nu \frac{(1-\gamma^5)}{2}\nu_l\big] \\
&= \frac{4G_F}{\sqrt{2}} V_{cb} \big[\bar{c}\gamma^\mu P_L b\big] \big[\bar{l}\gamma^\nu P_L \nu_l\big] \\
&= \frac{4G_F}{\sqrt{2}} V_{cb} O_{VL},
\end{aligned}$$

where $O_{V_L} = (\bar{c}\gamma_\mu P_L b)\,(\bar{\tau}\gamma^\mu P_L \nu)$. Thus the effective Hamiltonian for the quark level transition $b \to c\,\tau\,\bar{\nu}$ in the SM depends only on one operator, O_{VL}. Therefore, the effective Hamiltonian for $b \to c\,\tau\,\bar{\nu}$ transition in the SM is given by

$$H_{eff} = \frac{4G_F}{\sqrt{2}} V_{cb} O_{V_L}. \tag{2.50}$$

This quark level transition induces decays such as $B \to D\tau\,\bar{\nu}$, $B \to D^*\tau\,\bar{\nu}$ and $B_c \to J/\psi\;\tau\nu$.

The Feynman diagrams for $B \to D\tau\nu$ and $B \to D^*\tau\nu$ decays in the SM are depicted in the right panel of Fig. 2.8. The $B \to D^*\tau\nu$ vector and axial vector operator matrix elements, which depend on the

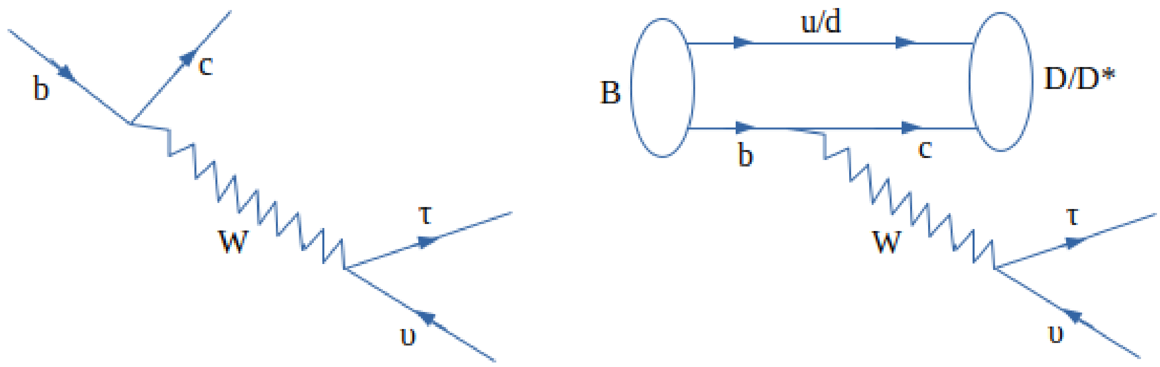

Figure 2.8: Feynman diagrams for $b \to c\,\tau\,\bar{\nu}$ transition (left) and $B \to D/D^*\,\tau\,\bar{\nu}$ decays (right) in the SM.

momentum transfer between B and D^*, can be expressed as

$$\begin{aligned} \langle D^*(k,\varepsilon)|\bar{c}\gamma_\mu b|\overline{B}(p)\rangle =& -i\epsilon_{\mu\nu\rho\sigma}\varepsilon^{\nu *}p^\rho k^\sigma \frac{2V(q^2)}{m_B + m_{D^*}}\,, \\ \langle D^*(k,\varepsilon)|\bar{c}\gamma_\mu\gamma_5 b|\overline{B}(p)\rangle =& \varepsilon^{\mu *}(m_B + m_{D^*})A_1(q^2) - (p+k)_\mu(\varepsilon^* q)\frac{A_2(q^2)}{m_B + m_{D^*}} \\ & - q_\mu(\varepsilon^* q)\frac{2m_{D^*}}{q^2}[A_3(q^2) - A_0(q^2)]\,, \end{aligned} \tag{2.51}$$

where

$$A_3(q^2) = \frac{m_B + m_{D^*}}{2m_{D^*}}A_1(q^2) - \frac{m_B - m_{D^*}}{2m_{D^*}}A_2(q^2)\,, \tag{2.52}$$

with $A_3(0) = A_0(0)$. The form factors V, A_0, A_1, A_2 can be written in terms of the heavy quark effective theory (HQET) form factors as [101, 168]

$$\begin{aligned} V(q^2) =& \frac{m_B + m_{D^*}}{2\sqrt{m_B m_{D^*}}}\,h_V(w(q^2))\,, \\ A_1(q^2) =& \frac{(m_B + m_{D^*})^2 - q^2}{2\sqrt{m_B m_{D^*}}(m_B + m_{D^*})}\,h_{A_1}(w(q^2))\,, \\ A_2(q^2) =& \frac{m_B + m_{D^*}}{2\sqrt{m_B m_{D^*}}}\left[h_{A_3}(w(q^2)) + \frac{m_{D^*}}{m_B}h_{A_2}(w(q^2))\right]\,, \\ A_0(q^2) =& \frac{1}{2\sqrt{m_B m_{D^*}}}\left[\frac{(m_B + m_{D^*})^2 - q^2}{2m_{D^*}}\,h_{A_1}(w(q^2)) \right. \\ & \left. - \frac{m_B^2 - m_{D^*}^2 + q^2}{2m_B}\,h_{A_2}(w(q^2)) - \frac{m_B^2 - m_{D^*}^2 - q^2}{2m_{D^*}}\,h_{A_3}(w(q^2))\right]\,, \end{aligned} \tag{2.53}$$

where the HQET form factors are given in [168].

The complete angular distribution of the decay $B \to D^*(\to D\pi)\,\tau\,\bar{\nu}$ in the presence of new physics can be parameterized in terms of four kinematic variables $\theta_D, \theta_\tau, \phi$ and q^2. Here θ_D is the angle between B and D mesons where D meson comes from D^* decay, θ_τ is the angle between τ and B and ϕ is the angle between D^* decay plane and the plane defined by the tau momenta whereas $q^2 = (p_B - p_{D^*})^2$, where p_B and p_{D^*} are the four momenta of B and D^* respectively.

The hadronic amplitudes in $B \to D\,\tau\,\bar{\nu}$ are defined as

$$H^{\lambda_D}_{V_{L,R},\lambda}(q^2) = \varepsilon^*_\mu(\lambda)\,\langle D(\lambda_D)|\bar{c}\gamma^\mu(1\mp\gamma_5)b|B\rangle\,,$$
$$H^{\lambda_D}_{S_{L,R},\lambda}(q^2) = \langle D(\lambda_D)|\bar{c}(1\mp\gamma_5)b|B\rangle\,,$$
$$H^{\lambda_D}_{T,\lambda\lambda'}(q^2) = -H^{\lambda_D}_{T,\lambda'\lambda}(q^2) = \varepsilon^*_\mu(\lambda)\varepsilon^*_\nu(\lambda')\,\langle D(\lambda_D)|\bar{c}\sigma^{\mu\nu}(1-\gamma_5)b|B\rangle\,. \tag{2.54}$$

where λ_D and λ denote the D meson and virtual intermediate boson helicities ($\lambda_D = s$ and $\lambda = 0, \pm1, t$) in the B rest frame, respectively. The nonzero amplitudes are given below.

$$H^s_{V,0}(q^2) = H^s_{V_L,0}(q^2) = H^s_{V_R,0}(q^2) = \sqrt{\frac{\lambda_D(q^2)}{q^2}}F_1(q^2),$$
$$H^s_{V,t}(q^2) = H^s_{V_L,t}(q^2) = H^s_{V_R,t}(q^2) = \frac{m_B^2 - m_D^2}{\sqrt{q^2}}F_0(q^2),$$
$$H^s_S(q^2) = H^s_{S_L}(q^2) = H^s_{S_R}(q^2) \simeq \frac{m_B^2 - m_D^2}{m_b - m_c}F_0(q^2),$$
$$H^s_T(q^2) = H^s_{T,+-}(q^2) = H^s_{T,0t}(q^2) = -\frac{\sqrt{\lambda_D(q^2)}}{m_B + m_D}F_T(q^2). \tag{2.55}$$

The three body decay $B \to D\,\tau\,\bar{\nu}$ can be studied by two independent parameters: (a) $q^2 = (p_B - p_D)^2$, where p_B and p_D are four momentum of B and D meson and (b) θ, the angle between the τ lepton momentum and the momentum of virtual boson in the rest frame of B meson. By integrating over θ, we can find the differential decay rate with respect to q^2. Using the effective Hamiltonian in Eq. (2.50) and calculating the helicity amplitudes [99], one can calculate the differential decay rate for $B \to D\,\tau\,\bar{\nu}$ decay [101].

Recently several groups have updated the theoretical predictions of the ratios R_D and R_{D^*} (ratios of decay rates of $B \to D^{(*)}\,\tau\,\bar{\nu_\tau}$ and $B \to D^{(*)}\,(e/\mu)\,\bar{\nu}$) using different approaches, see for e.g., refs. [169–172]. Ref. [169] improved the SM prediction of R_D by making use of the lattice calculations of $B \to D\,l\,\bar{\nu}$ form factors [173, 174] along with stronger unitarity constraints. The value of R_{D^*} has been updated in [170] by performing a combined fit to the $B \to D^{(*)}\,l\,\bar{\nu}$ decay distributions and including uncertainties in the form factor ratios at $\mathcal{O}(\alpha_s,\,\Lambda_{\rm QCD}/m_{c,b})$ in HQET. Ref. [171] obtained the SM prediction for R_{D^*} by using heavy quark symmetry relations between the form factors and including recent inputs from lattice calculations and experiments. The SM prediction for R_{D^*} was obtained in [172] by including the available known corrections at $\mathcal{O}(\alpha_s,\,\Lambda_{\rm QCD}/m_{c,b})$ in the HQET relations between the form factors along with the unknown corrections in the ratios of the HQET form factors. This was done by introducing additional factors and fitting them from the experimental data and various lattice inputs.